Membrane currents in cultured human intestinal smooth muscle cells

A. V. Zholos, C. J. Fenech, S. A. Prestwich and T. B. Bolton

Department of Pharmacology and Clinical Pharmacology, St George's Hospital Medical School, London SW17 ORE, UK

(Received 1 June 2000; accepted 19 July 2000)

1. Using whole-cell patch-clamp recording techniques, we have examined voltage-gated ion currents in a cultured human intestinal smooth muscle cell line (HISM). Experiments were performed at room temperature on cells after passages 16 and 17.

2. Two major components of the whole-cell current were a tetraethylammonium-sensitive ($IC_{50} = 9$ mM), iberiotoxin-resistant, delayed rectifier K^+ current and a Na^+ current inhibited by tetrodotoxin ($IC_{50} \approx 100$ nM). No measurable inward current via voltage-gated Ca^{2+} channels could be detected in these cells even with 10 mM Ca^{2+} or Ba^{2+} in the external solution. No current attributable to calcium-activated K^+ channels was found and no cationic current in response to muscarinic receptor activation was present.

3. In divalent cation-free external solution two additional currents were activated: an inwardly rectifying hyperpolarization-activated current, I_{HA}, and a depolarization-activated current, I_{DA}.

4. I_{HA} and I_{DA} could be carried by several monovalent cations; the sizes of currents in descending order were: $K^+ > Cs^+ > Na^+$ for I_{HA} and $Na^+ > K^+ \gg Cs^+$ for I_{DA}. I_{HA} was activated and deactivated instantaneously and showed no inactivation whereas I_{DA} was activated, inactivated and deactivated within tens of milliseconds. These currents were inhibited by external calcium with an IC_{50} of 0.3 μM for I_{DA} and an IC_{50} of 20 μM for I_{HA}.

5. Cyclopiazonic acid (CPA) induced an outward, but not an inward current. SK&F 96365, a blocker of store-operated Ca^{2+} channels, suppressed I_{DA} with a half-maximal inhibitory concentration of 9 μM but was ineffective in inhibiting I_{HA} at concentrations up to 100 μM. Gd^{3+} and La^{3+} strongly suppressed I_{DA} at 1 and 10 μM, respectively and were less effective in blocking I_{HA} (complete inhibition required a concentration of 100 μM for both). Carbachol at 10–100 μM evoked about a 3-fold increase in I_{HA} amplitude and completely abolished I_{DA}.

6. We conclude that I_{HA} and I_{DA} are Ca^{2+}-blockable cationic currents with different ion selectivity profiles that are carried by different channels. I_{DA} shows novel voltage-dependent properties for a cationic current.

It is well known that several distinct cellular phenotypes may exist during normal smooth muscle ontogenesis; in contrast to skeletal and cardiac muscle cells, which exhibit much more restricted cellular plasticity, mature smooth muscle cells can readily dedifferentiate from the contractile phenotypic state to a non-contractile (highly proliferative, migratory and synthetic) phenotype where synthesis of a connective tissue matrix and proliferation occur (for reviews see Chamley-Campbell *et al.* 1979; Owens, 1995), thus reverting to a more primitive phenotype in culture. This process involves considerable morphological, electrophysiological and biochemical changes and is thought to be crucial for normal smooth muscle myogenesis as well as for pathogenesis. It has recently been shown that cultured gastrointestinal smooth muscle cells also may retain distinct molecular phenotypes which, depending on the initial cell density, substrate specificity and serum supplementation, have been suggested to be identical to those *in vivo* (Brittingham *et al.* 1998). It thus appears that cultured cells recapitulate a significant part of *in vivo* smooth muscle ontogenesis. Substantial electrophysiological changes possibly relevant to the proliferation process have also been described (e.g. Snetkov *et al.* 1996).

In the present study we examined the properties of voltage-dependent inward and outward currents in cultured human intestinal smooth muscle (HISM) cells (American Type Culture Collection, ATCC no. 1692-CRL). This established cell line is widely used in biochemical and molecular biology research but data

concerning the electrophysiological properties of HISM cells are scarce. The major inward current, which we identified as a 'classical' fast, TTX-sensitive Na^+ current with properties similar to those of cells freshly dispersed from the adult human colon (Xiong *et al.* 1993), was previously erroneously referred to as Ca^{2+} current via L-type channels despite its very rapid inactivation kinetics (Bielefeldt *et al.* 1996). Also, we found two distinct Ca^{2+}-blockable inward cationic currents to be present in these cells, which could be elicited in divalent cation-free external solution. One of these, I_{HA}, was further potentiated by the muscarinic agonist carbachol via muscarinic receptor/G-protein activation since the effect was blocked by atropine or intracellular GDP-βS application. The other current, which we termed I_{DA}, showed a pronounced U-shaped I–V relationship at negative potentials with a peak at about −30 mV. However, in contrast to the muscarinic cationic current widely present in differentiated gastrointestinal smooth muscles, I_{DA} also showed pronounced inactivation. These two currents also had distinct pharmacological profiles.

We could not identify in HISM cells a muscarinic cationic current with a typical U-shaped voltage dependence as seen in all studied gastrointestinal smooth muscle cells from various non-human mammalian species (e.g. Benham *et al.* 1985; Inoue & Isenberg, 1990; Zholos & Bolton, 1994). From the above considerations it remains to be established whether such a current, although normally expressed in mature human smooth muscle cells, is lost during the dedifferentiation process in culture. Arresting cell growth by using serum-free conditions for up to 19 days also failed to induce such a current in HISM cells.

METHODS

Cell culture

HISM cells (ATCC no. 1692-CRL) were cultured in Dulbecco's modified Eagle's medium (DMEM) with high glucose (Gibco-BRL), supplemented with 10% fetal calf serum (FCS), 100 u ml^{-1} penicillin (Gibco-BRL) and 100 u ml^{-1} streptomycin. For electrophysiology, cells were treated with 0.25% trypsin (Gibco-BRL) for 1 min at 37 °C, collected by centrifugation, resuspended in fresh medium, plated on glass coverslips and left to attach for about 10 min. Cells were used after passages 16 and 17.

Electrical recordings and data analysis

Whole-cell membrane current was recorded at room temperature using low-resistance borosilicate patch pipettes (1–3 MΩ) and an Axopatch 200A (Axon Instruments Inc.) voltage-clamp amplifier. Voltage-clamp pulses were generated and data were captured using a Digidata 1200 interfaced to a computer running the pCLAMP 6 program (Axon Instruments Inc.). Series resistance was compensated (usually by about 80%) to produce the fastest transient without oscillations. For sodium current (I_{Na}) recordings the signal was filtered (4-pole low-pass Bessel filter) at 5 kHz and sampled at 40 kHz; for cationic current these settings were 1 and 5 kHz, respectively. No leak correction was used in either case. Data were analysed and plotted using MicroCal Origin version 5.0 software (MicroCal Software, Inc., Northampton, MA, USA). Values are given as means ± S.E.M.

Solutions

The basic external physiological salt solution (PSS) used to maintain the cells before giga-seal formation consisted of (mM): NaCl 120, KCl 6, $CaCl_2$ 2.5, $MgCl_2$ 1.2, glucose 12 and Hepes 10, pH adjusted to 7.4 with NaOH. For I_{Na} recordings KCl was replaced by NaCl (total Na^+ concentration, 130 mM) and $MgCl_2$ was removed. Cationic currents were measured in solutions to which $CaCl_2$ was not added. In ion substitution experiments NaCl was replaced with equimolar KCl, CsCl or *N*-methyl-D-glucamine chloride (NMDG-Cl; pH adjusted with KOH, CsOH or HCl, respectively). To study the dependency of the cationic current on $[Ca^{2+}]_o$, extracellular calcium was strongly buffered to 36 and 487 nM using Ca^{2+}/EGTA mixtures (4 mM/10 mM and 9 mM/10 mM, respectively). For higher concentrations, 250 μM or 1 mM $CaCl_2$ was added to nominally divalent cation-free solution.

Complete exchange of the external solution was achieved within about 1 s as described previously (Zholos & Bolton, 1995).

Pipettes were filled with the following solution (mM): CsCl 80, MgATP 1, creatine 5, glucose 20, Hepes 10, BAPTA 10 and $CaCl_2$ 4.6 ($[Ca^{2+}]_i = 100$ nM), pH adjusted to 7.4 with CsOH (total Cs^+ concentration, 124 mM). GTP (1 mM) was added in some experiments where the effects of carbachol were studied. NaCl (10 mM) was added in experiments where I_{Na} was measured to define the sodium equilibrium potential (E_{Na}). In experiments to measure K^+ currents, the pipette solution contained (mM): KCl 130, MgATP 1, creatine 5, glucose 20, Hepes 10 and EGTA 0.05, pH adjusted to 7.4 with NaOH.

Chemicals used

Tetrodotoxin (TTX), tetraethylammonium chloride (TEA-Cl), adenosine 5′-triphosphate (ATP, magnesium salt), guanosine 5′-triphosphate (GTP, sodium salt), guanosine-5′-*O*-(2-thiodiphosphate (GDPβS, trilithium salt), cyclopiazonic acid (CPA), creatine, Hepes, BAPTA, EGTA, NMDG-Cl, carbamylcholine chloride (carbachol) and atropine were obtained from Sigma Chemical Co. SK&F 96365 was obtained from Biomol Research Laboratories, Inc. (Plymouth Meeting, PA, USA). All other chemicals were from BDH Laboratory Supplies (AnalaR grade; Poole, Dorset, UK).

RESULTS

Whole-cell membrane currents

Experiments were performed on 122 human cultured intestinal cells from passages 16–17. In 11 cells studied using basic external PSS and K^+-based, low-EGTA pipette solution, voltage pulses applied from either −50 or −100 mV evoked time-independent currents the size of which was a linear function of the test potential between −90 and about 0 mV. These presumably 'leak' currents indicated an input resistance of about 3 GΩ. At more positive potentials an outward current was activated and reached a peak in about 20–100 ms in the voltage range 0–90 mV, respectively (Fig. 1). The current was reversibly inhibited by TEA^+ with an IC_{50} of 9.0 ± 0.1 mM ($n = 3$) and it was also abolished when K^+ was replaced by Cs^+ in the pipette solution. Thus, the current could be tentatively identified as a delayed rectifier K^+ current. No spontaneous transient outward current (STOC)-like activity (Bolton *et al.* 1999), characteristic of smooth muscle cells of various origins, was seen in HISM cells. Moreover, caffeine (10 mM) or carbachol (50 μM) application even at depolarized or positive potentials (e.g. +10 mV) did not activate any

outward currents. Since ryanodine- and carbachol-sensitive intracellular Ca^{2+} stores are functional in these cells (Bielefeldt *et al.* 1997), these results suggest the absence or a very low expression level of Ca^{2+}-activated K^+ channels. Furthermore, iberiotoxin (IbTX), a potent and selective inhibitor of large conductance Ca^{2+}-activated K^+ (BK_{Ca}) channels, had no effect on I_K (Fig. 1, bottom left). In four cells I_K amplitude at +100 mV in the presence of 300 nM IbTX was 94 ± 10% of control ($P < 0.05$).

The outward current evoked from a holding potential of −50 mV was not affected by shifting the holding potential to −100 mV. However, an initial fast transient inward current appeared. To isolate and characterize this current in the experiments described below, K^+ in the pipette and external solutions was replaced by Cs^+ and Na^+, respectively.

TTX-sensitive Na^+ current

An inward current with rapid activation/inactivation kinetics was seen in all cells studied. However, its maximal amplitude greatly varied (from −670 to −5315 pA at +10 mV from a holding potential of −100 mV) with no obvious relation to cell size. The mean value was 2.3 ± 0.2 nA ($n = 24$), which corresponded to a current density of 20 ± 2 pA pF^{-1}. The cell membrane capacitance was on average 127 ± 8 pF ($n = 67$).

Replacing external Na^+ with Cs^+ completely abolished the inward current even though either 10 mM Ca^{2+} or 10 mM Ba^{2+} was present in the external solution (Fig. 2*A* and *B*). The current was also abolished by replacing Na^+ with K^+ or $NMDG^+$ (not shown).

There are two major classes of voltage-dependent Na^+ channel, TTX-sensitive and TTX-resistant channels. TTX was added to the external solution in a cumulative manner at concentrations ranging from 0.1 nM to 1 μM while I_{Na} was measured at 10 s intervals (Fig. 2*C*). TTX at 1 nM slightly reduced the current; at 1 μM the current was inhibited almost completely (superimposed current traces in Fig. 2*D*). The IC_{50} value was 56 nM (Fig. 2*E*; mean 96 ± 21 nM, $n = 3$).

Superimposed TTX-sensitive currents obtained by subtracting current traces in the presence of 1 μM TTX

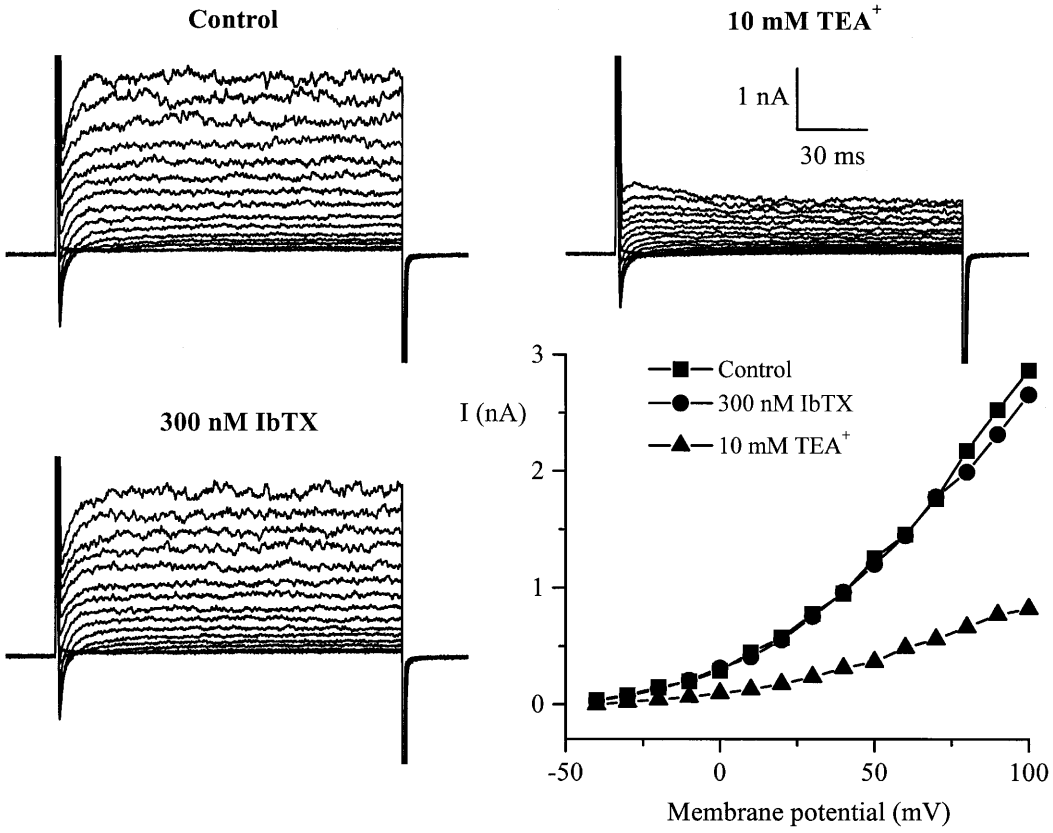

Figure 1. Whole-cell membrane currents in HISM cells under quasiphysiological conditions

Families of superimposed whole-cell currents in a single cultured HISM cell evoked by 150 ms voltage pulses applied at 10 s intervals from a holding potential of −100 mV to test potentials between −40 and +100 mV with a 10 mV increment in control and in the presence of 10 mM TEA^+ or 300 nM IbTX. *I–V* relationships were constructed by measuring the peak amplitude of the outward current at each test potential. High-K^+ pipette solution and normal PSS in the bath were used.

from those in control are shown in Fig. 3*A*. Voltage pulses were applied from −100 mV to test potentials ranging from −70 to +90 mV in 5 mV increments. Measurable inward current was activated at about −30 mV, reached a peak value at +10 mV and reversed at +68 mV, very close to the E_{Na} of +65 mV ($[Na^+]_i$ was 10 mM; Fig. 3*B*). The activation and inactivation kinetics accelerated with membrane depolarization. Thus, the time to peak exponentially decreased from 12 to 2 ms in the range −30 to +30 mV. The decay time constant decreased from about 10 to 2.5 ms at potentials from −10 to +30 mV, respectively. At more negative potentials where the current was too small for reliable fitting or could not be measured directly, a conventional double-pulse protocol revealed an inactivation process with time constants in the range 25–14 ms at potentials from −50 to −20 mV, respectively (not shown). Overall the time constant decreased e-fold with depolarization by 37 mV.

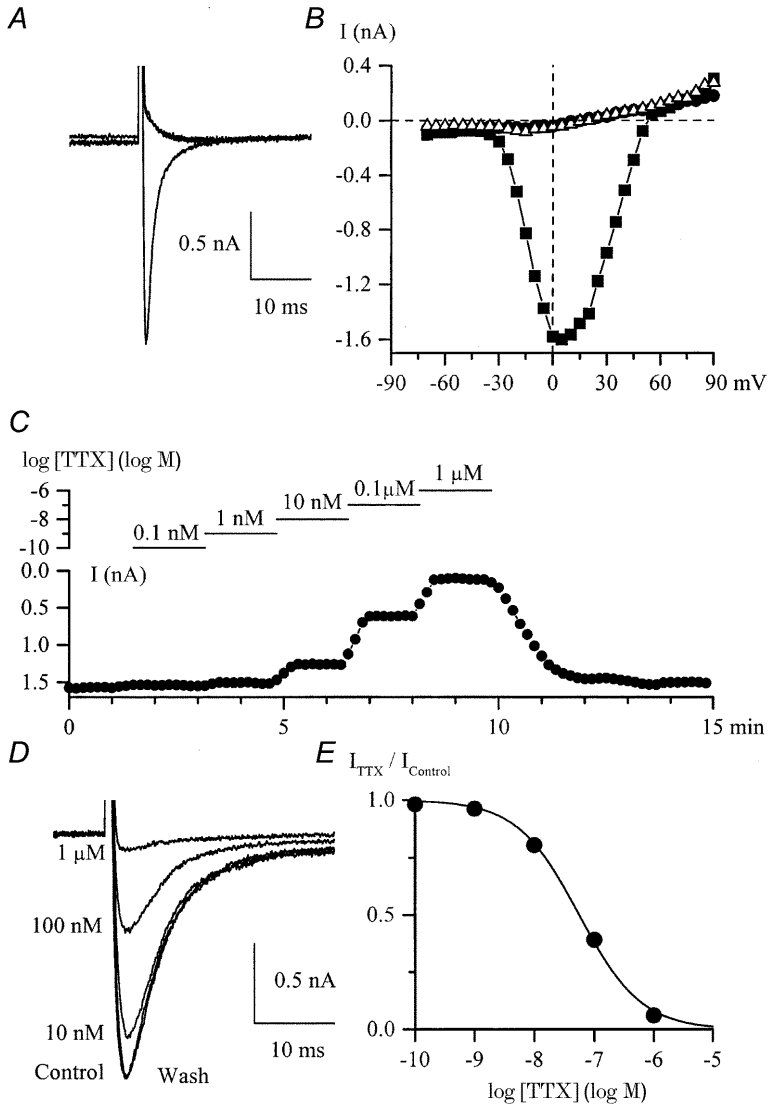

Figure 2. Inward currents in a single cultured HISM cell

A, superimposed current traces elicited by depolarizing pulses to 0 mV from −100 mV in control (135 mM Na^+, 2.5 mM Ca^{2+}) and after replacement of Na^+ by Cs^+ (125 mM) with 10 mM $CaCl_2$ or $BaCl_2$ added to the external solution. *B*, *I–V* relationships for the peak inward current in control (■) and high-Cs^+ external solution with 10 mM Ca^{2+} (●) or 10 mM Ba^{2+} (△) in the same cell. *C*, peak inward Na^+ current was measured at +10 mV by applying voltage steps from −100 mV every 10 s upon cumulative application of ascending concentrations of TTX as shown by the horizontal lines on the logarithmic concentration scale. External solutions contained Na^+ and Ca^{2+} but not Mg^{2+}. *D*, examples of I_{Na} from the same experiment. The concentrations of TTX applied are indicated. *E*, concentration–effect curve for the experiment illustrated in *C* and *D*. Data points represent relative current ($I_{TTX}/I_{Control}$) fitted by the logistic function with an IC_{50} value of 56 nM. I_{TTX} is the current in TTX.

Peak sodium conductance was estimated by dividing the peak current amplitude by the driving force ($E - E_{Na}$, where E is the membrane potential) at each test potential (Fig. 3*C*). The half-activation potential ($V_{1/2}$) was found to be -3.2 ± 1.4 mV and the slope factor (k) was -6.7 ± 1.0 mV ($n = 19$). The activation kinetics of the Na^+ current was not analysed, but assuming an m^3 process (e.g. $G/G_{max} = m^3$, where G_{max} is the maximal conductance and the activation parameter m obeys the Boltzmann distribution), the $V_{1/2}$ and k values could be estimated to be −13.1 and −9.4 mV, respectively, for the example shown in Fig. 3*C*.

The steady-state inactivation of the current was assessed by holding the membrane potential at different values between −120 and −15 mV for 10 s followed by a voltage step to +10 mV. Superimposed current traces obtained with this protocol are shown in Fig. 3*D*. Plotting the peak

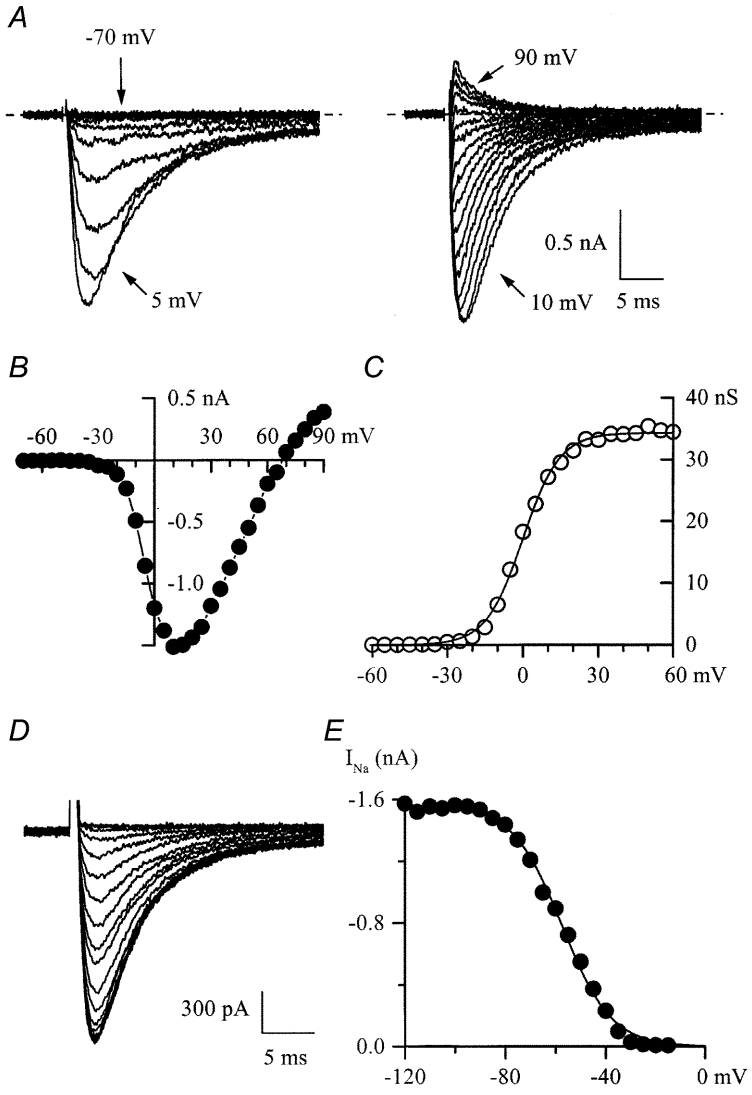

Figure 3. Voltage-dependent properties of TTX-sensitive inward Na^+ current in external solution with Ca^{2+} but no Mg^{2+}

A, superimposed current traces obtained by paired subtraction of currents after 1 μM TTX application from those in control. The holding potential was −100 mV; 30 ms voltage steps were applied to test potentials ranging from −70 to +5 mV (left) and from +10 to +90 mV (right) in 5 mV increments. *B*, *I–V* relationship for the peak I_{Na} shown in *A*. *C*, activation curve obtained by dividing the peak current amplitude by the driving force at each test potential ($E - E_{Na}$, where $E_{Na} = +65$ mV) and fitted by a Boltzmann function with the following best fit parameters: maximal conductance, $G_{max} = 34$ nS; potential of half-maximal activation, $V_{1/2} = 0$ mV; slope factor, $k = -7.3$ mV. *D*, superimposed current traces elicited by 25 ms voltage steps to +10 mV applied from various holding potentials (−120 to −15 mV in 5 mV increments). *E*, steady-state inactivation of I_{Na} for the experiment illustrated in *D*. Data points were fitted by a Boltzmann function with a potential of half-maximal inactivation of −57.4 mV and a slope factor of 9.8 mV.

current as a function of the preceding holding potential (e.g. Fig. 3*E*) revealed a half-inactivation potential of -61.9 ± 2.2 mV and a slope factor of 9.5 ± 0.6 mV ($n = 10$).

Recovery from inactivation was measured by applying a 70 ms depolarizing pulse to +10 mV followed by a short test pulse to +10 mV with a variable delay (Fig. 4*A*, bottom trace). The recovery process could be well described by a single exponential function (dashed line in Fig. 4*A*; see also Fig. 4*B*). There was an e-fold change in the time constant per 15.7 mV in the example shown in Fig. 4*B* and *C*. On average the time constant describing the recovery process increased e-fold per 17.3 ± 4.2 mV ($n = 4$).

Cationic currents

When the external solution was changed to a divalent cation-free, 130 mM Na^+ solution two additional currents were observed. The voltage protocol used was either a series of steps from −40 mV to potentials between +100 and −180 mV as in Fig. 5*A* and *B* or a slow voltage ramp in the same range as shown schematically in Fig. 6*A* (bottom). The first current was inwardly rectifying with instantaneous activation and deactivation kinetics and no obvious inactivation except at very positive potentials (Fig. 5*A* and *B*). Voltage steps and slow voltage ramps produced very similar *I–V* relationships (Fig. 5*C*, circles and continuous lines, respectively). We termed this hyperpolarization-activated current I_{HA}. A second current was seen upon a voltage step to −40 mV from a more negative test potential as in Fig. 5*B* or following the voltage ramp as in Fig. 6*A*. We termed this depolarization-activated current I_{DA}. It showed rapid inactivation kinetics and thus might have been interpreted as a tail current due to the deactivation of the inwardly rectifying conductance, but further experiments showed that this was not the explanation. Both currents progressively increased in size with time after divalent cation removal (Fig. 6*B*, top panel). However, the time course of their increases was different.

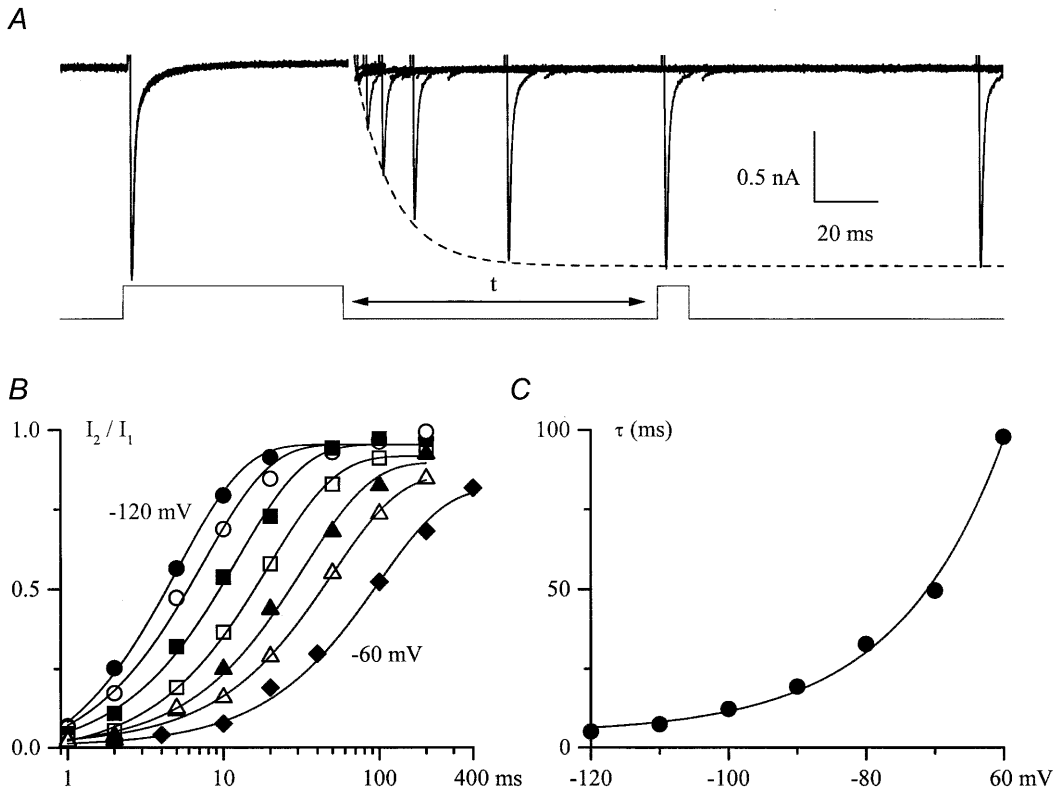

Figure 4. Recovery of I_{Na} from inactivation

A, I_{Na} elicited by a 70 ms prepulse and a 10 ms test pulse to +10 mV applied from −100 mV with a variable interpulse interval, *t* (as shown below). Capacitance transients have been removed for clarity. Peak I_{Na} during the recovery process could be well fitted by a single exponential function with a time constant of 12.3 ms as shown by the dashed line. *B*, relative I_{Na} plotted against interpulse interval on a semilogarithmic scale at different membrane potentials (from left to right, −120 to −60 mV in 10 mV increments) and fitted by single exponential functions as shown by the continuous lines. *C*, voltage dependence of the time constant characterizing I_{Na} recovery from inactivation in a single experiment, fitted by a single exponential function with an e-fold increase in τ per 15.7 mV.

The inwardly rectifying current reached a maximum 75 s after external divalent cation removal (e.g. Fig. 6*B*, top panel, circles) whereas in the same cell the current seen upon the voltage step to −40 mV continued to increase in size and stabilized in different cells after about 100–200 s (e.g. Fig. 6*B*, top panel, triangles). Furthermore, the dependence of I_{HA} and I_{DA} on the external calcium concentration was different. The currents stabilized 50 s after Ca^{2+} readmission to the external solution. I_{DA} was inhibited with an IC_{50} of 311 nM whereas for I_{HA} the IC_{50} value in the same cell was 20 μM and the concentration–effect curve was less steep (Fig. 6*B*, bottom). These observations indicated that the currents were not related. Overall statistics for the occurrence of these currents in different cells also supported this conclusion. Thus, in experiments with Na^+ or K^+ as the main cation in the external solution, in only 35% of cells studied (14 out of 40) were the two currents observed simultaneously. I_{HA} was present in the majority of these cells whereas I_{DA} was seen less frequently (in 35 and 16 out

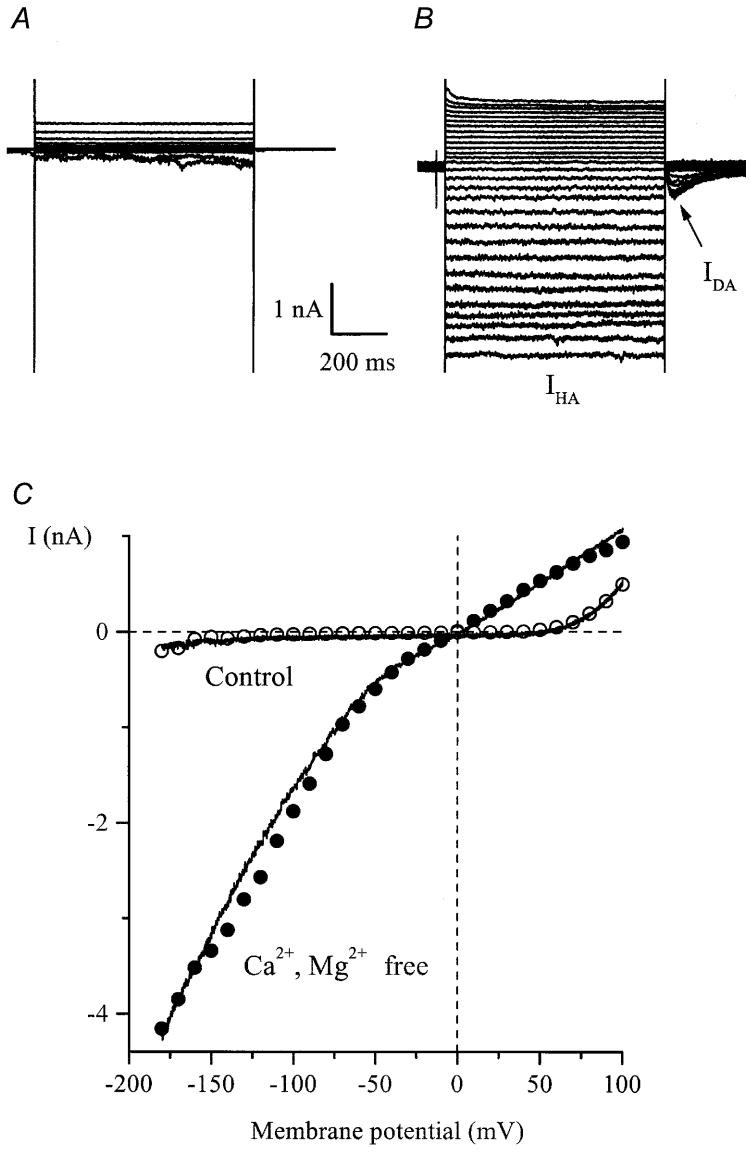

Figure 5. Inward currents in cultured HISM cells developing in divalent cation-free external solution

A and *B*, superimposed current traces elicited by 800 ms duration voltage steps from −40 mV to test potentials between +100 and −180 mV in 10 mV increments in control (130 mM Na^+, 2.5 mM Ca^{2+}, 1.2 mM Mg^{2+}; *A*) and after external Ca^{2+} and Mg^{2+} removal (*B*, denoted as I_{HA}). Note the instantaneous activation and deactivation of I_{HA} as well as the noisy appearance of the current at negative potentials. The current seen upon repolarization to −40 mV is denoted as I_{DA}. *C*, *I–V* relationships for currents measured at the end of the pulse (○ and ●) and, in the same cell, by applying 1 s duration voltage ramps from +100 to −180 mV (continuous lines). The ramp protocol is illustrated in Fig. 6*A*.

of 40 cells studied, respectively). In 20 cells studied using Cs^+ as the main external cation, I_{DA} was undetectable whereas I_{HA} was seen in 19 cells. These observations implied different ion selectivity of the channels underlying these currents. To investigate this further, ion substitution experiments were performed. In the experiments illustrated in Fig. 6*C* and *D*, 130 mM Na^+ in the external solution was replaced by equimolar amounts of Cs^+, K^+ or $NMDG^+$. The sizes of the current in the different solutions were in the following descending order: $K^+ > Cs^+ > Na^+$ for I_{HA} (Fig. 6*C*) and $Na^+ > K^+ \gg Cs^+$ for I_{DA} (Fig. 6*D*). Similar results were obtained from five cells. Substitution with the large impermeable $NMDG^+$ cation completely abolished both I_{HA} (Fig. 6*C*; note that control current was recorded in Na^+ solution containing 2.5 mM Ca^{2+}) and I_{DA} (Fig. 6*D*; note the small inward current in control solution, Na^+ with 2.5 mM Ca^{2+}, compared to the $NMDG^+$-based solution). Moreover, the reversal potential was close to 0 mV and remained almost the same: +5.5 mV with Na^+,

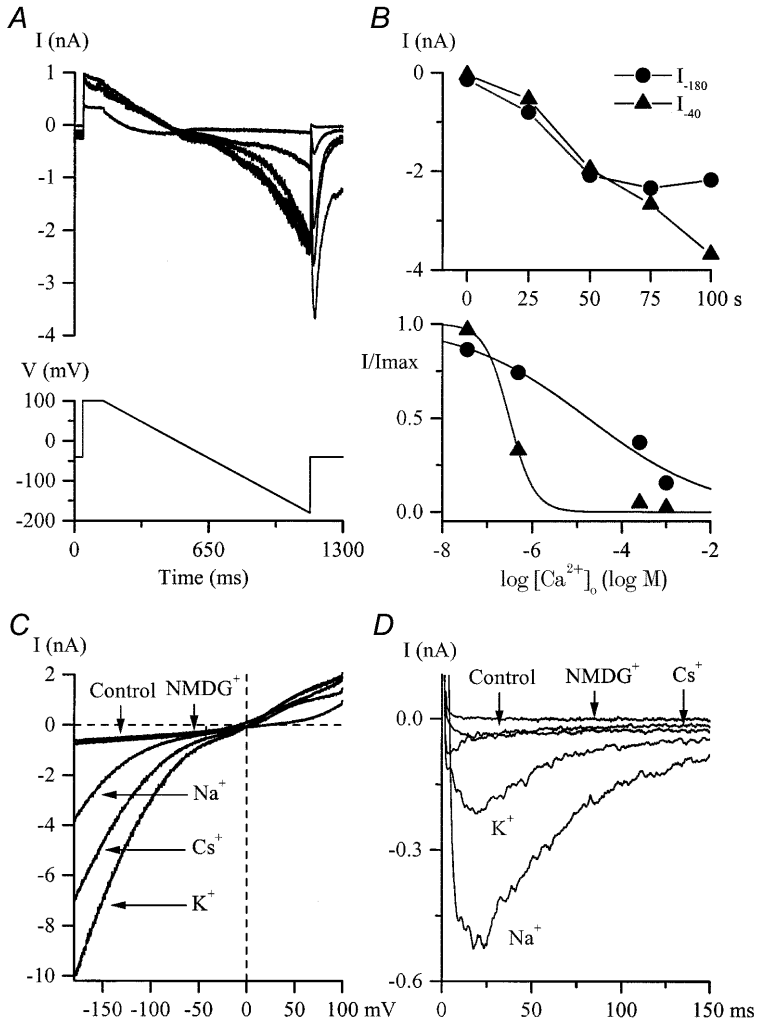

Figure 6. Kinetics, $[Ca^{2+}]_o$ dependence and ion permeation properties of I_{HA} and I_{DA}

A, typical currents during a slow voltage ramp from +100 to −180 mV and a voltage step to −40 mV slowly developing after Ca^{2+} and Mg^{2+} removal from the external solution. Superimposed current traces were recorded at 25 s intervals. *B*, top, maximal amplitudes of inward currents at −180 mV (●, I_{HA}) and at −40 mV after the ramp (▲, I_{DA}) plotted against time where time zero represents the moment of Ca^{2+} and Mg^{2+} removal from the external solution. Bottom, dependence of I_{HA} (●) and I_{DA} (▲) in the same cell on the external free Ca^{2+} concentration. Relative currents were fitted by logistic functions with IC_{50} values of 20 μM for I_{HA} and 311 nM for I_{DA}. *C* and *D*, external cation substitution experiments were performed on two different cells after I_{HA} (*C*) and I_{DA} (*D*) had been stabilized in a divalent cation-free external solution. The control *I–V* relationship for I_{HA} (voltage protocol as in *A*) and control current response for I_{DA} (voltage step from −100 to −40 mV) were obtained in high-Na^+, 2.5 mM $CaCl_2$-containing external solution. Traces labelled 'Na^+' were obtained after Ca^{2+} removal whereas all other traces were obtained in solutions with Na^+ replacement as described in the Methods. High-Cs^+ pipette solution was used.

+3.3 mV with Cs^+ and +2.6 mV with K^+ in the external solution. In three cells expressing I_{HA} alone, changing the pH of the external solution from 7.4 to 6.4 or 8.4 had almost no effect on the amplitude of the current or its reversal potential (data not shown).

The above results clearly indicate that I_{HA} and I_{DA} are carried via distinct cation channels which differ in their relative permeabilities to Na^+, K^+ and Cs^+ and in their voltage and extracellular Ca^{2+} dependence.

Pharmacological properties of I_{HA} and I_{DA} cationic currents

It is now well established that a variety of cationic channels are commonly expressed in various smooth muscles. The gating events which open these channels are also diverse and include membrane stretch, Ca^{2+} release and/or a rise in $[Ca^{2+}]_i$, receptor and G-protein activation, a change in membrane polarization, protein kinase C activation, etc. Our observation that I_{HA} and I_{DA} were activated by Ca^{2+} removal from the external solution indicated a crucial role of external Ca^{2+} in the channel gating. A wide variety of cell types respond to external Ca^{2+} removal by generating cationic currents or non-selective currents carried by both cations and anions. The known examples include epithelium (Van Driessche & Zeiske, 1985; Desmedt *et al.* 1993), skeletal muscle (Almers *et al.* 1984), chick embryo ectoderm (Li *et al.* 1994), cardiac muscle (Mubagwa *et al.* 1997) and *Xenopus* oocytes (Zhang *et al.* 1998).

Another possibility was that in Ca^{2+}-free external solution the intracellular stores could be passively depleted and this could account for the slow development of I_{HA} and I_{DA} due to the opening of calcium release-activated channels (CRACs). Thus, we performed experiments to see whether Ca^{2+} store depletion could induce such currents *per se*.

In these cultured intestinal smooth muscle cells both ryanodine- and $InsP_3$-sensitive Ca^{2+} stores have been identified and the cholinergic agonist carbachol has been shown to release Ca^{2+} from both pools (Oh *et al.* 1997; Bielefeldt *et al.* 1997). Thus, we tested further the effects of carbachol. In the presence of Ca^{2+}, carbachol application induced no or a very small inward current. It is also interesting to note here that the delayed rectifier K^+ current was strongly inhibited by carbachol (by 60% at 50 μM); the inhibition was voltage independent between 0 and +80 mV. Such an effect has been previously demonstrated in freshly isolated gastric myocytes (Lammel *et al.* 1991) as well as for the cloned smooth muscle-derived delayed rectifier potassium channels (Vogalis *et al.* 1995).

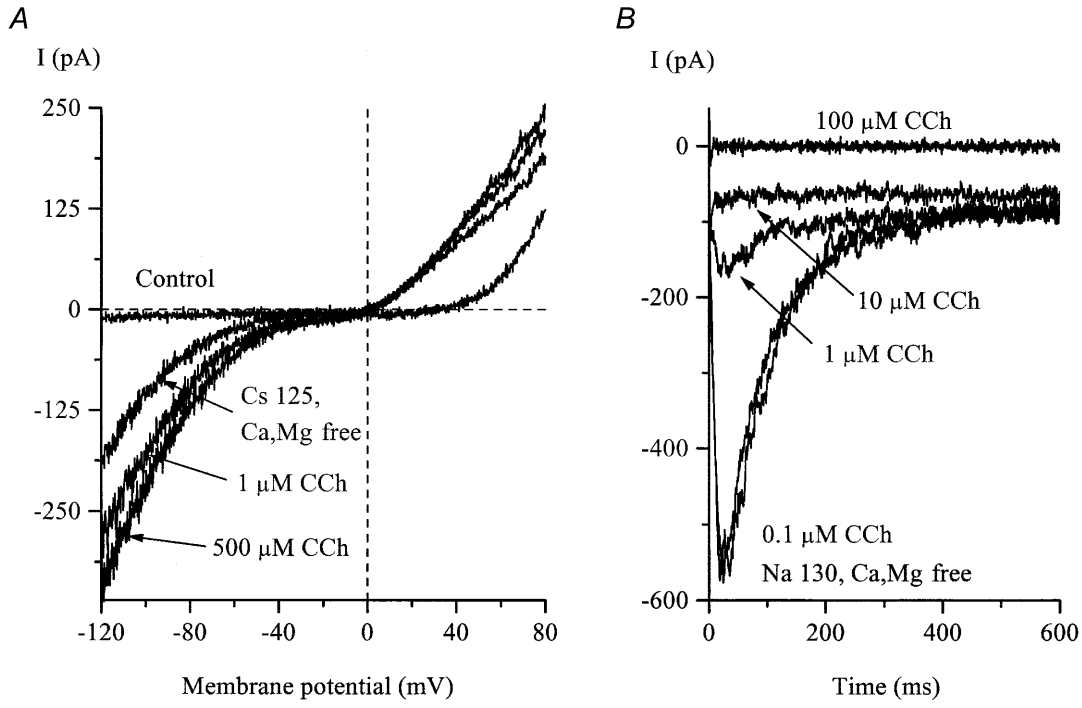

Figure 7. Effects of carbachol on I_{HA} and I_{DA}

A, the control *I–V* relationship was measured as described for Fig. 6*C*. After I_{HA} had developed in divalent cation-free, high-Cs^+ external solution, it was rapidly potentiated by carbachol (CCh) application. I_{DA} was abolished in Cs^+-containing external solution and was inactivated at −40 mV. *B*, in a different cell, I_{DA} measured at −40 mV in divalent cation-free, high-Na^+ external solution was strongly inhibited by carbachol.

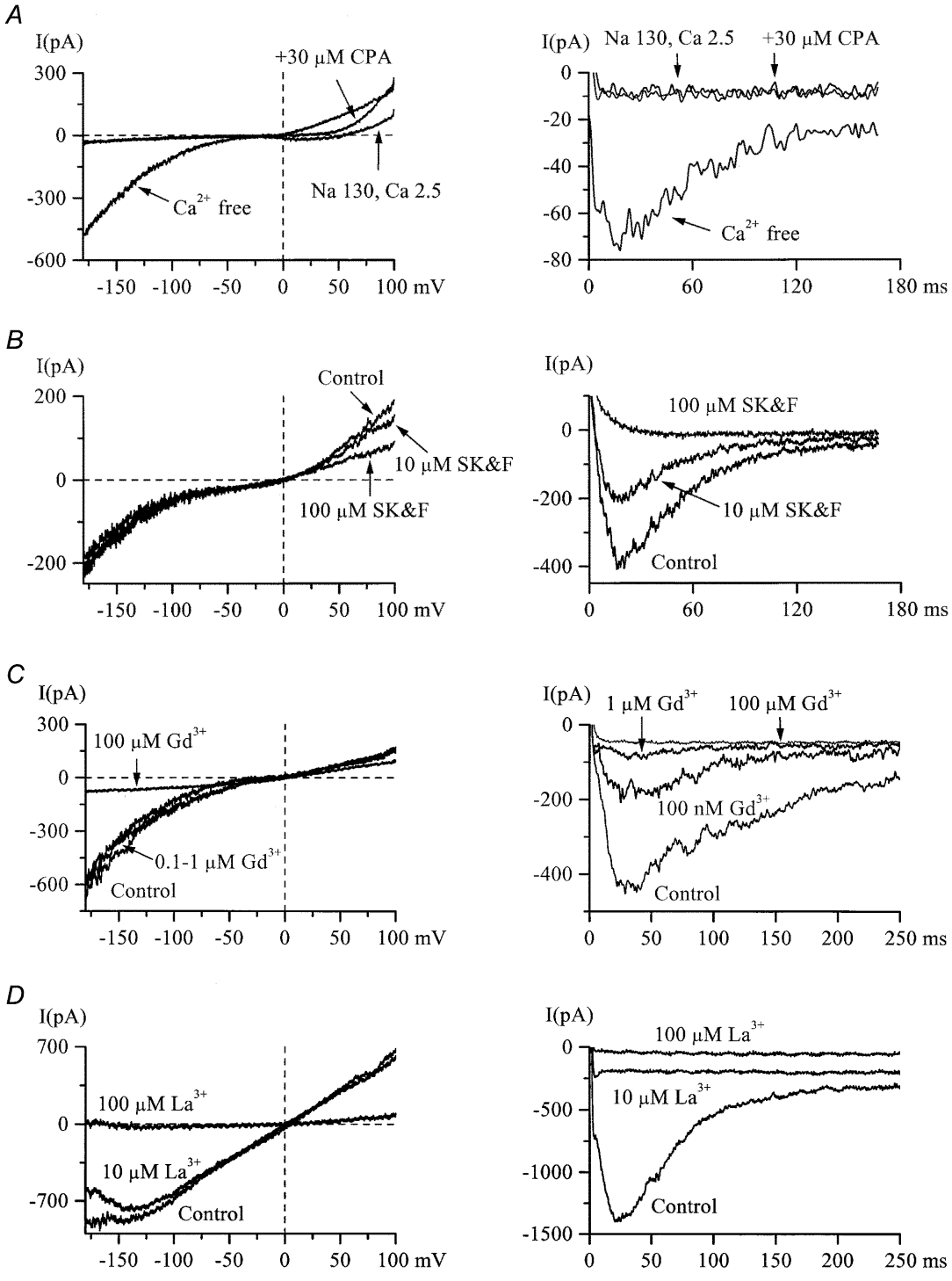

Figure 8. Pharmacological properties of I_{HA} and I_{DA}

A, 5 min treatment with 30 μM CPA failed to induce an inward I_{HA} (left) or I_{DA} (right) in 2.5 mM Ca^{2+}, high-Na^+ external solution ($n = 5$), but both currents were readily activated following Ca^{2+} removal. Note that at positive potentials current could be activated by CPA. *B*, SK&F 96365 at concentrations of up to 100 μM did not inhibit inward I_{HA} (left), but completely abolished I_{DA} (right) in the same cell ($n = 7$). Current at positive potentials at which it could be activated by CPA (left panel in *A*) was also inhibited by SK&F 96365. *C* and *D*, I_{DA} (right) was more sensitive to the inhibitory action of Gd^{3+} or La^{3+} compared to I_{HA} (left) but both currents were abolished by 100 μM of either blocker. In all panels I_{HA} and I_{DA} were measured in the same cells.

However, after I_{HA} had developed in Ca^{2+}-free solution, it was rapidly increased by carbachol application in a dose-dependent manner; carbachol at 1 μM was nearly maximally effective (Fig. 7*A*). The amplitude of I_{HA} in the presence of saturating agonist concentrations (10–100 μM) relative to that before carbachol application was 2.77 ± 0.50 ($n = 5$). The effect of carbachol was practically abolished in the presence of 1 μM atropine (ratio of amplitudes, 1.09 ± 0.05 ($n = 4$) with and without atropine plus 10 μM carbachol) or in cells where GDPβS (2 mM) was allowed to diffuse into the cell from the pipette solution for about 5 min to inhibit G-proteins prior to carbachol application (there was little increase in I_{HA}; the ratio of amplitudes in these cells was 1.06 ± 0.08 ($n = 4$) with 10 μM carbachol). Thus, both effects were statistically significant ($P < 0.03$; two-tailed unpaired t test) indicating the involvement of muscarinic receptors/G-proteins in the signal transduction pathways. As mentioned above, I_{DA} occurred very infrequently but in two cells where this current was present the same carbachol concentrations (10–100 μM) strongly inhibited and finally abolished I_{DA} (one example is shown in Fig. 7*B*).

Cyclopiazonic acid (CPA), an inhibitor of the sarco-(endo)plasmic reticulum Ca^{2+} pump (SERCA), is widely used as a pharmacological tool to deplete intracellular Ca^{2+} stores. In four cells tested, application of CPA at 30 μM for 5–8 min failed to induce inward cationic currents when Ca^{2+} was present in the external solution but both currents could be readily induced in the same cells in Ca^{2+}-free solution (Fig. 8*A*). Thus, it appeared that Ca^{2+} store depletion alone, if this was an underlying mechanism, was insufficient for I_{HA} or I_{DA} activation as the channels are primarily controlled (suppressed) by external calcium ions. It was also notable in all cells tested that CPA did induce an outward current. Its amplitude at very positive potentials was the same as that of I_{HA} during subsequent Ca^{2+}-free solution application (Fig. 8*A*).

SK&F 96365, a blocker of store-operated Ca^{2+} channels (Clementi & Meldolesi, 1996), suppressed I_{DA} with a half-maximal inhibitory concentration of 9 μM but was ineffective in blocking inward I_{HA} at concentrations up to 100 μM (Fig. 8*B*). Interestingly, an outward current at the same potentials at which it could be induced by CPA was inhibited by SK&F 96365. Also, at 100 μM SK&F 96365 almost completely blocked the TTX-sensitive Na^+ current; the inhibition was reversible ($\tau_{on} = 7.5$ s; $\tau_{off} = 103$ s).

Gadolinium and lanthanum are useful pharmacological tools as antagonists of mechano-sensitive (e.g. stretch- or

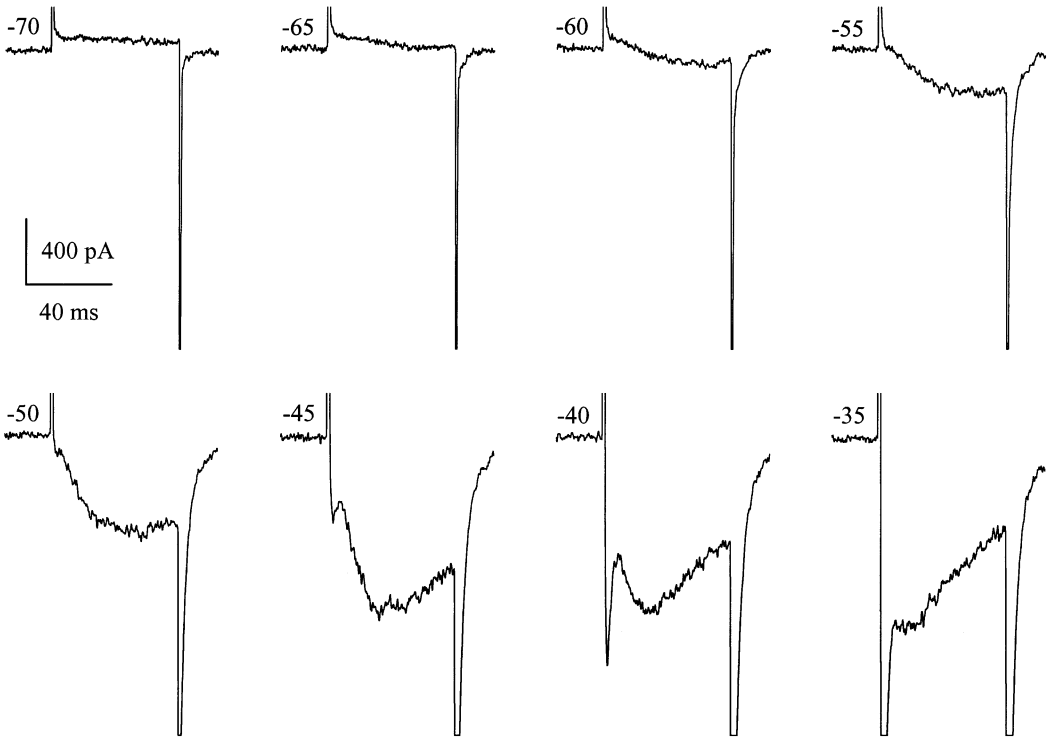

Figure 9. Amplitude and kinetic relationships between I_{Na} and I_{DA}

Current traces were recorded in a high-Na^+, divalent cation-free solution upon voltage steps from −100 mV to various test potentials indicated beside each trace. I_{HA} was 160, 122 and 81 pA at −100, −70 and −35 mV, respectively.

swelling-activated) cationic channels (Hamill & McBride, 1996), as well as external Ca^{2+}-blockable cationic channels (Van Driessche *et al.* 1988; Mubagwa *et al.* 1997; Zhang *et al.* 1998). In 13 HISM cells tested, I_{DA} was found to be more sensitive to the blocking action of Gd^{3+} and La^{3+} compared to I_{HA}, the latter being completely inhibited only at 100 μM (Fig. 8*D*).

Voltage-dependent properties of I_{DA}

Since I_{DA} showed steady-state inactivation properties very similar to those for I_{Na} in these cells (see Fig. 10*C*) we also considered the possibility that modulation of Na^+ channel gating in Ca^{2+}-free solution could somehow be involved (Armstrong, 1999; Armstrong & Cota, 1999). However, TTX at 1 μM had no effect on I_{DA}. This current was also distinct from I_{Na} in its kinetics and voltage dependence of activation. Figure 9 shows current traces

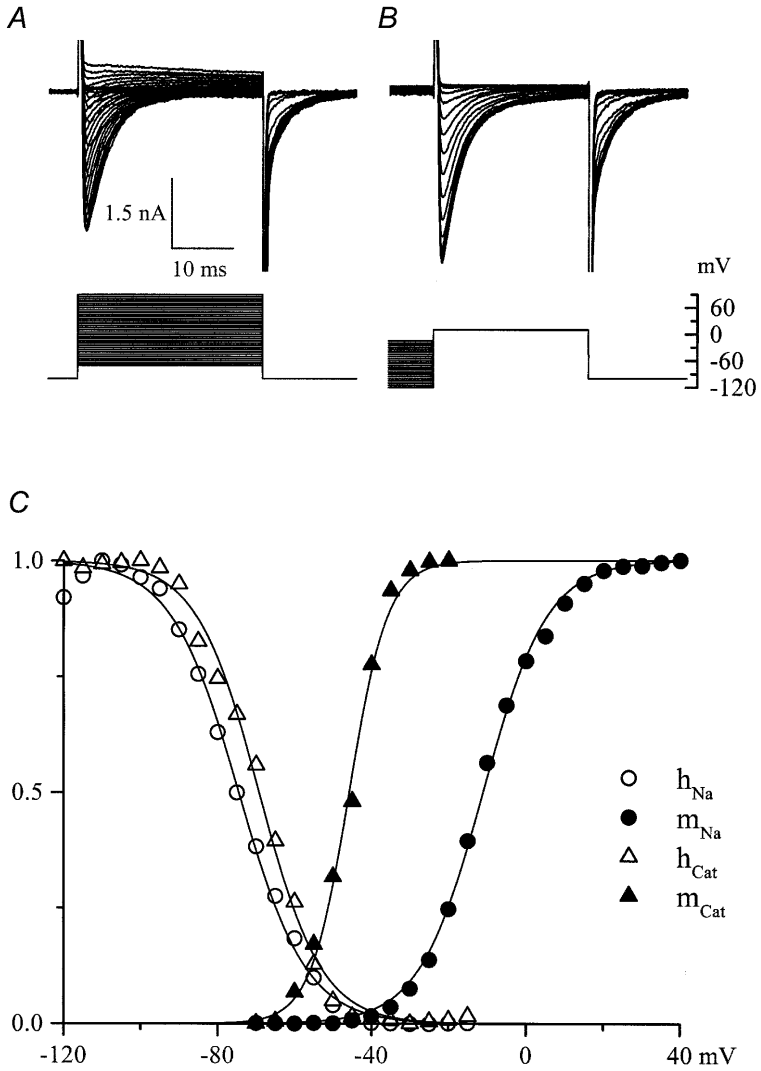

Figure 10. Comparison of the voltage dependence of activation and inactivation of I_{Na} and I_{DA}

A and *B*, families of superimposed current traces and voltage protocols used to study the voltage dependence of activation (*A*) and inactivation (*B*). Measurements were made of I_{Na} at its peak and activation of I_{DA} 30 ms after stepping to various potentials from a holding potential of −100 mV; at 30 ms I_{Na} is largely inactivated (cf. Fig. 3) but I_{DA} is close to its peak value. In *B* the test potential was +10 mV, close to the reversal potential (V_{rev}) for I_{DA}, thus minimizing its contribution during measurements of I_{Na} inactivation. Again, a 30 ms pulse allows I_{Na} to inactivate leaving I_{DA} close to its peak value. *C*, open and filled circles show, respectively, normalized I_{Na} amplitude from *B* (h_{Na}) and relative Na^+ conductance calculated from I_{Na} amplitudes in *A* (m_{Na}) as described for Fig. 3*C*, respectively. Filled and open triangles show relative tail current amplitudes from *A* (m_{Cat}) and *B* (h_{Cat}), respectively, measured by fitting single exponential functions and extrapolating to time zero at the end of each test pulse. Data points were fitted by Boltzmann functions with the following best fit parameters: I_{Na} activation: $V_{1/2} = -11.1$ mV; $k = -8.3$ mV; I_{Na} inactivation: $V_{1/2} = -74.5$ mV, $k = 8.8$ mV; I_{DA} activation: $V_{1/2} = -45.8$ mV, $k = -5.0$ mV; I_{DA} inactivation: $V_{1/2} = -69.2$ mV, $k = 8.1$ mV. This cell was in 130 mM Na^+, divalent cation-free solution; I_{HA} was small (−145 and +155 pA at −100 and +90 mV, respectively).

recorded in high-Na^+, divalent cation-free external solution upon stepping from the holding potential of −100 mV to various levels indicated beside each current trace. Activation of I_{DA} occurred at potentials more negative than activation of I_{Na} (e.g. −60 mV). Since I_{DA} activation was much slower than that of I_{Na} these currents produced two distinct peaks (e.g. between −45 and −35 mV). The rate of I_{DA} inactivation was also considerably slower. At more positive test potentials, I_{DA} was masked by a generally much larger I_{Na}. Thus, to study the voltage dependence of its activation and inactivation we employed the protocols shown schematically in Fig. 10*A* and *B*, respectively. These voltage-dependent parameters for I_{DA} were assessed by measuring tail current amplitude at −100 mV after voltage steps to different test potentials (activation; Fig. 10*A*) or after a voltage step to +10 mV applied from different holding potentials (inactivation; Fig. 10*B*). The amplitude of the tail current was measured by fitting a single exponential function with extrapolation to the beginning of repolarization. Normalized values are shown in Fig. 10*C* by triangles, with open symbols for inactivation and filled symbols for activation. For comparison, steady-state activation and inactivation curves for I_{Na} in the same cell are also shown; these were obtained as described above (e.g. Fig. 3). Steady-state inactivation for the two currents was surprisingly similar both in the slope and in the position on the voltage axis (only 5 mV difference in the $V_{1/2}$ values). However, the activation curve for I_{DA} was steeper and positioned about 35 mV more negative than that for I_{Na}. Thus, a small steady I_{DA} ('window current') can be generated in the voltage range −60 to −30 mV under conditions when Ca^{2+} stores are depleted (compare to Fig. 9).

The position of the activation curve for I_{DA} on the voltage axis is very similar to that for the muscarinic cationic conductance in guinea-pig ileal smooth muscle cells (compare with Inoue & Isenberg, 1990; Zholos & Bolton, 1994). Given that both currents are cation currents, I_{DA} might be expected to show a similar U-shaped *I–V* relationship. In the experiment illustrated in Fig. 11*A*, I_{DA} was measured by applying voltage steps from

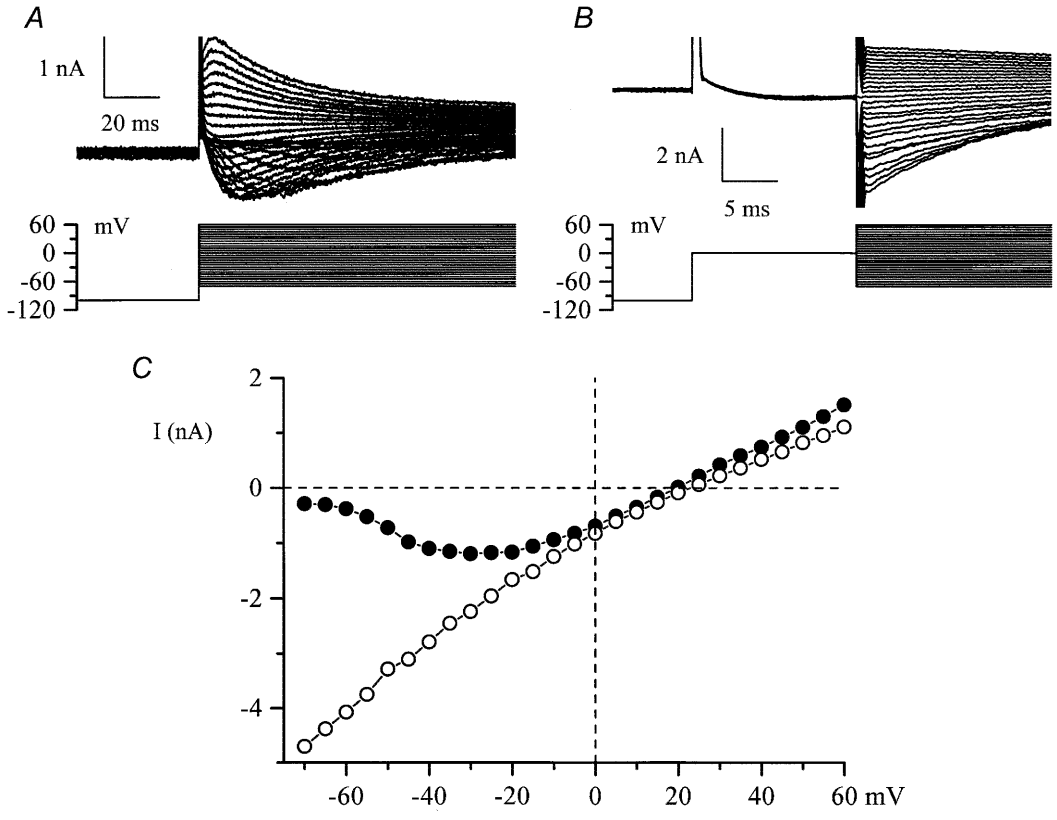

Figure 11. *I–V* relationships for I_{DA}

A and *B*, voltage protocols and superimposed current traces recorded in the same cultured HISM cell using high-Cs^+ pipette and high-K^+, divalent cation-free external solution in which I_{Na} is abolished and I_{DA} can be measured. I_{HA} was relatively small in this cell: measured by applying voltage ramps from −40 mV to inactivate I_{DA}, I_{HA} amplitude was −427 pA at −70 mV and 315 pA at +60 mV. In *B* steps were in the range −70 to +60mV. Tail current was flat at +20 mV. *C*, *I–V* relationships for the peak I_{DA} in *A* (●) and instantaneous tail current amplitude in *B* (○), measured as described for Fig. 10*B*. Tail current reversed at +23 mV which was 3 mV more positive than the peak I_{DA} reversal potential. This discrepancy could arise as a result of some contamination of the peak I_{DA} by I_{HA}, as explained above, for which $V_{rev} \approx 0$ mV.

−100 mV to various test potentials. The instantaneous I–V relationship for this current was also evaluated in the same cell by stepping to 0 mV (maximal activation) followed by voltage steps to between −70 and +60 mV (Fig. 11*B*). Figure 11*C* compares I–V relationships obtained using these protocols. The instantaneous I–V relationship (○) is nearly linear implying an almost linear dependence of single channel current amplitude on the membrane potential (constant single channel conductance), whereas peak I_{DA} showed a bell-shaped voltage dependence (●) declining almost to the zero level at very negative potentials (compare with Fig. 5 of Inoue & Isenberg, 1990). The reversal potential in the two cases was nearly the same.

DISCUSSION

Smooth muscle cell cultures offer a valuable approach to study the mechanisms and potential regulatory pathways controlling cell differentiation (Owens, 1995). However, substantial modification of cell properties means that careful studies are required in each particular case and the results obtained may not represent *in vivo* properties of fully differentiated cells. In the present patch-clamp study we investigated the electrophysiological behaviour of cultured HISM cells, which until now were poorly characterized.

The lack of voltage-gated Ca^{2+} channels (Fig. 2*A* and *B*) in these cells is clearly the result of altered properties of cultured HISM cells as compared with their native counterparts. The L-type channel proteins are ubiquitously expressed in all freshly isolated gastrointestinal smooth muscle cells studied, including human jejunal and colonic myocytes (Farrugia *et al.* 1995; Xiong *et al.* 1995). It must be noted that in a previous study the inward current in cultured HISM cells was erroneously identified as a voltage-gated Ca^{2+} current via L-type Ca^{2+} channels despite its atypical rapid inactivation for such a current. No ion substitution tests were performed and this conclusion was drawn from the partial inhibition by nifedipine (20 μM) and verapamil (Bielefeldt *et al.* 1996). In our experiments this fast inward current persisted in a Ca^{2+}-free external solution (e.g. Figs 9 and 10) and was abolished in Na^+-free solutions (replacement by Cs^+, K^+ or $NMDG^+$; e.g. Figs 2*A* and 11*A*). Moreover, the current was TTX sensitive ($IC_{50} \approx 100$ nM). Many different smooth muscle cells normally express both Ca^{2+} channels and voltage-gated, TTX-sensitive Na^+ channels (e.g. rat ileum, Smirnov *et al.* 1992; for review see Kuriyama *et al.* 1998). Na^+ channels may also be expressed in cultured smooth muscle cells, usually in a relatively minor population of cells, even though they are not observed in their native counterparts (e.g. Snetkov *et al.* 1996). TTX-sensitive Na^+ channels were present in all HISM cells tested though I_{Na} greatly varied in amplitude with no obvious relation to cell size. It is interesting to note that arresting cell growth by using serum-free conditions for up to 19 days did not abolish I_{Na} but substantially accelerated its inactivation kinetics; for example at +10 mV the decay time constant decreased from 5.2 to 0.9 ms (data not shown).

The overall properties of I_{Na} in cultured HISM cells appear very similar to those in freshly isolated human colonic myocytes except for an approximately 7-fold higher IC_{50} value for TTX (Xiong *et al.* 1993). In both cases the currents peaked at about 0 mV and inactivated within about 10 ms. The availability curves had similar slopes and $V_{1/2}$ values but the activation curve in HISM was positioned 19 mV more positive in HISM cells compared to native cells without any significant change in the voltage dependence (slopes, 6.7 *vs.* 7.6 mV, respectively). There was also a clear indication of the overexpression of Na^+ channels in cultured cells as the current density on average was 20 times higher compared to that of freshly isolated human cells (Xiong *et al.* 1993).

BK_{Ca} channels are ubiquitously expressed in visceral smooth muscles giving rise to STOC discharge or large outward currents in response to intracellular Ca^{2+} release (Bolton *et al.* 1999). In cultured HISM cells both ryanodine- and InsP_3-sensitive Ca^{2+} stores are functional (Oh *et al.* 1997), but under conditions of low intracellular Ca^{2+} buffering we observed neither STOCs nor outward currents in response to caffeine or carbachol. This suggests that BK_{Ca} channels are not expressed in these cells, which is further confirmed by the lack of block by IbTX (Fig. 1). However, it is unlikely that these channels are lost in culture since in cells freshly dispersed from human jejunum, Ca^{2+}-dependent K^+ channels are also lacking. The major difference was in the activation range for the TEA^+-sensitive K^+ current, which was about 60 mV more positive in cultured cells compared to freshly isolated jejunal cells (Farrugia *et al.* 1993).

Upon carbachol application, even at high concentrations, muscarinic receptor cationic current, I_{CAT}, with a characteristic U-shaped voltage dependence was not observed in HISM cells. Since in guinea-pig ileal cells I_{CAT} is strongly inhibited by external divalent cations (Zholos & Bolton, 1995), Ca^{2+} and Mg^{2+} were removed in an attempt to unmask this current. Though I_{CAT} was not revealed under these conditions we found two other cationic currents previously not seen in freshly dissociated smooth muscle cells. Under divalent cation-free conditions they developed very slowly and initially almost in parallel (Fig. 6*A* and *B*). At later times the current termed I_{HA} stabilized whereas the other current, termed I_{DA}, continued to increase. This was the first indication that different ion channels mediate these two currents. I_{DA} turned out to be much more sensitive to $[Ca^{2+}]_o$ (Fig. 6*B*). The channels also had different ion-selectivity profiles and different voltage-dependent and pharmacological properties.

The slow appearance of the currents in divalent cation-

free medium could indicate the involvement of passive Ca^{2+} store depletion in their generation. Thus, the channels could be potentially related to CRACs through which capacitative refilling of Ca^{2+} stores is believed to occur. This has been found to be a dominant Ca^{2+} entry pathway in a large variety of cells, particularly in non-excitable cells (reviewed by Parekh & Penner, 1997). Store-operated Ca^{2+} influx has also been reported in cultured smooth muscle cells such as A7r5 vascular cells (Blatter, 1995; Byron & Taylor, 1995) and the DDT1MF-2 cell line (Ufret-Vincenty *et al.* 1995).

I_{CRAC} is difficult to measure directly in smooth muscle cells. However, recent studies on other cell types have established that monovalent cation outward currents can be generated by CRACs even when Ca^{2+} is present in the external solution (Hoth, 1996). When the external free Ca^{2+} concentration was reduced to micromolar levels in the absence of Mg^{2+}, I_{CRAC} in Jurkat T-cells was significantly increased (Lepple-Wienhues & Cahalan, 1996) and single CRAC conductance for Na^+ was much higher compared to the Ca^{2+} current through CRACs (Kerschbaum & Cahalan, 1999). Using CPA, a sarco-endoplasmic reticulum Ca^{2+} pump (SERCA) inhibitor, to deplete the store we found that an outward current developed and the same component of the current was inhibited by SK&F 96365, a blocker of store-operated Ca^{2+} channels (Fig. 8*A* and *B*). However, beyond this there were more differences than similarities between I_{HA} and I_{DA} in HISM cells and I_{CRAC} in other cells. To summarize, it appears that some properties of a CRAC current are shared with I_{HA} (e.g. voltage dependence, kinetics, inward rectification, the lack of inactivation in Ca^{2+}-free solution, similar IC_{50} values for inhibition by external Ca^{2+}, effects of carbachol) whereas other properties are shared with I_{DA} (e.g. the blocking action of Gd^{3+}, La^{3+} and SK&F 96365, and the sequence of conductance $Na^+ > K^+ \gg Cs^+$ is identical to that in Jurkat T cells). Thus, an amplified CRAC component may be present in divalent cation-free solution but the properties of neither I_{HA} nor I_{DA} are the same as those described for I_{CRAC} in other cell types.

Since no stimulation of the cells was employed (e.g. mechanical stimuli or agonists) to evoke these currents, the remaining possibility is that I_{HA} and I_{DA} belong to the family of Ca^{2+}-blockable cationic currents which appear to be ubiquitous in various cell types but so far have not been described in smooth muscle cells. The opening of such channels is believed to produce the membrane depolarization commonly occurring in Ca^{2+}-free solutions and two mechanisms have been proposed to explain this phenomenon.

One possibility is that the removal of external Ca^{2+} alters the selectivity and/or gating properties of Ca^{2+} or Na^+ channels (e.g. Almers *et al.* 1984; Armstrong, 1999; Armstrong & Cota, 1999). In HISM cells this seems unlikely since Ca^{2+} channels are absent and TTX did not affect the cationic currents. The voltage-dependent availability curves for I_{Na} and I_{DA} were strikingly similar (Fig. 10*C*), but other properties were different and it is an important observation that all three currents could be observed in the same cell. Moreover, I_{Na} was abolished in K^+ solutions but both cationic currents remained.

The other possibility is that Ca^{2+} removal unmasks cationic channels (e.g. Van Driessche & Zeiske, 1985; Mubagwa *et al.* 1997). Activation of hemi-gap-junctional channels has recently been implicated in *Xenopus* oocytes (Zhang *et al.* 1998), but these channels are permeable to anions and even to large organic monovalent cations such as $NMDG^+$, which is clearly not the case in HISM cells (e.g. Fig. 6*C* and *D*). Also, the voltage dependence and channel kinetic properties of HISM cells and oocytes are different.

In ventricular myocytes, Mubagwa *et al.* (1997) described a novel Ca^{2+}-blockable cationic current with properties remarkably similar to those of I_{HA} in HISM cells. The current was blocked by Ca^{2+} with an IC_{50} of 60 μM (compare to 20 μM for I_{HA}). Thus, the authors postulated the existence of a high-affinity binding site for Ca^{2+} at or near the extracellular site of the cationic channel, so that the slow off-rate could explain the slow development ($>$ 5 min) of the current, which is also the case for I_{HA}. I_{DA} developed even more slowly, consistent with an even lower apparent dissociation constant for Ca^{2+} of about 0.3 μM. I_{HA} and cationic current in cardiac cells both show inward rectification, and have a very similar noisy appearance, amplitude and instantaneous activation/deactivation during voltage jumps (compare our Fig. 5*B* with Fig. 2*A* in Mubagwa *et al.* 1997). Both currents could be carried by monovalent cations in the same sequence $K^+ > Cs^+ > Na^+ \gg NMDG^+$, but not by Cl^-, and were abolished in the presence of 100 μM Gd^{3+}.

The physiological relevance of such a conductance in cells *in vivo* exposed to $[Ca^{2+}]_o$ in the millimolar range remains largely unclear. However, in cardiac cells there is a difference in the $[Ca^{2+}]_o$ sensitivity between intact tissue and single cells. Also, Mubagwa *et al.* (1997) raised the possibility that these channels can be physiologically regulated by agonists (though they did not observe any response to β-adrenergic or muscarinic receptor stimulation) or change their calcium sensitivity under pathophysiological conditions such as ischaemia or 'Ca^{2+} paradox'. Our findings that carbachol application can strongly potentiate I_{HA} via a muscarinic receptor/G-protein pathway support this hypothesis. Our first demonstration of I_{HA} in smooth muscle cells also shows that such a current is not tissue specific. Moreover, I_{DA} in HISM cells is a novel Ca^{2+}-blockable cationic current with no resemblance to previously described currents. Thus, even in the same cell distinct channels can mediate cationic fluxes in divalent cation-free solutions but their physiological function remains to be defined. HISM cells may provide a useful experimental model for future

studies since these channels, like Na^+ channels, are apparently overexpressed in these cultured cells, explaining why such currents were not previously found in freshly isolated smooth muscle cells.

Almers, W., McCleskey, E. W. & Palade, P. T. (1984). A non-selective cation conductance in frog muscle membrane blocked by micromolar external calcium ions. *Journal of Physiology* **353**, 565–583.

Armstrong, C. M. (1999). Distinguishing surface effects of calcium ion from pore-occupancy effects in Na^+ channels. *Proceedings of the National Academy of Sciences of the USA* **96**, 4158–4163.

Armstrong, C. M. & Cota, G. (1999). Calcium block of Na^+ channels and its effect on closing rate. *Proceedings of the National Academy of Sciences of the USA* **96**, 4154–4157.

Benham, C. D., Bolton, T. B. & Lang, R. J. (1985). Acetylcholine activates an inward current in single mammalian smooth muscle cells. *Nature* **316**, 345–347.

Bielefeldt, K., Waite, L., Abboud, F. M. & Conklin, J. L. (1996). Nongenomic effects of progesterone on human intestinal smooth muscle cells. *American Journal of Physiology* **271**, G370–376.

Bielefeldt, K., Whiteis, C. A., Sharma, R. V., Abboud, F. M. & Conklin, J. L. (1997). Reactive oxygen species and calcium homeostasis in cultured human intestinal smooth muscle cells. *American Journal of Physiology* **272**, G1439–1450.

Blatter, L. A. (1995). Depletion and filling of intracellular calcium stores in vascular smooth muscle. *American Journal of Physiology* **268**, C503–512.

Bolton, T. B., Prestwich, S. A., Zholos, A. V. & Gordienko, D. V. (1999). Excitation-contraction coupling in gastrointestinal and other smooth muscles. *Annual Review of Physiology* **61**, 85–115.

Brittingham, J., Phiel, C., Trzyna, W. C., Gabbeta, V. & McHugh, K. M. (1998). Identification of distinct molecular phenotypes in cultured gastrointestinal smooth muscle cells. *Gastroenterology* **115**, 605–617.

Byron, K. L. & Taylor, C. W. (1995). Vasopressin stimulation of Ca^{2+} mobilization, two bivalent cation entry pathways and Ca^{2+} efflux in A7r5 rat smooth muscle cells. *Journal of Physiology* **485**, 455–468.

Chamley-Campbell, J., Campbell, G. R. & Ross, R. (1979). The smooth muscle cell in culture. *Physiological Reviews* **59**, 1–61.

Clementi, E. & Meldolesi, J. (1996). Pharmacological and functional properties of voltage-independent Ca^{2+} channels. *Cell Calcium* **19**, 269–279.

Desmedt, L., Simaels, J. & Van Driessche, W. (1993). Ca^{2+}-blockable, poorly selective cation channels in the apical membrane of amphibian epithelia. Tetracaine blocks the UO_2^{2+}-insensitive pathway. *Journal of General Physiology* **101**, 103–116.

Farrugia, G., Rae, J. L., Sarr, M. G. & Szurszewski, J. H. (1993). Potassium current in circular smooth muscle of human jejunum activated by fenamates. *American Journal of Physiology* **265**, G873–879.

Farrugia, G., Rich, A., Rae, J. L., Sarr, M. G. & Szurszewski, J. H. (1995). Calcium currents in human and canine jejunal circular smooth muscle cells. *Gastroenterology* **109**, 707–717.

Hamill, O. P. & McBride, D. W. Jr (1996). The pharmacology of mechanogated membrane ion channels. *Pharmacological Reviews* **48**, 231–252.

Hoth, M. (1996). Depletion of intracellular calcium stores activates an outward potassium current in mast and RBL-1 cells that is correlated with CRAC channel activation. *FEBS Letters* **390**, 285–288.

Inoue, R. & Isenberg, G. (1990). Effect of membrane potential on acetylcholine-induced inward current in guinea-pig ileum. *Journal of Physiology* **424**, 57–71.

Kershbaum, H. H. & Cahalan, M. D. (1999). Single-channel recording of a store-operated Ca^{2+} channel in Jurkat T lymphocytes. *Science* **283**, 836–839.

Kuriyama, H., Kitamura, K., Itoh, T. & Inoue, R. (1998). Physiological features of visceral smooth muscle cells, with special reference to receptors and ion channels. *Physiological Reviews* **78**, 811–920.

Lammel, E., Deitmer, P. & Noack, T. (1991). Suppression of steady membrane currents by acetylcholine in single smooth muscle cells of the guinea-pig gastric fundus. *Journal of Physiology* **432**, 259–282.

Lepple-Wienhues, A. & Cahalan, M. D. (1996). Conductance and permeation of monovalent cations through depletion-activated Ca^{2+} channels (I_{CRAC}) in Jurkat T cells. *Biophysical Journal* **71**, 787–794.

Li, J. Q., Prod'hom, B. & Kucera, P. (1994). Cation channel blocked by extracellular Ca^{2+} in the apical membrane of the chick embryonic ectoderm. *Pflügers Archiv* **429**, 183–192.

Mubagwa, K., Stengl, M. & Flameng, W. (1997). Extracellular divalent cations block a cation non-selective conductance unrelated to calcium channels in rat cardiac muscle. *Journal of Physiology* **502**, 235–247.

Oh, S. T., Yedidag, E., Conklin, J. L., Martin, M. & Bielefeldt, K. (1997). Calcium release from intracellular stores and excitation-contraction coupling in intestinal smooth muscle. *Journal of Surgical Research* **71**, 79–86.

Owens, G. K. (1995). Regulation of differentiation of vascular smooth muscle cells. *Physiological Reviews* **75**, 487–517.

Parekh, A. B. & Penner, R. (1997). Store depletion and calcium influx. *Physiological Reviews* **77**, 901–930.

Smirnov, S. V., Zholos, A. V. & Shuba, M. F. (1992). Potential-dependent inward currents in single isolated smooth muscle cells of the rat ileum. *Journal of Physiology* **454**, 549–571.

Snetkov, V. A., Hirst, S. J. & Ward, J. P. T. (1996). Ion channels in freshly isolated and cultured human bronchial smooth muscle cells. *Experimental Physiology* **81**, 791–804.

Ufret-Vincenty, C. A., Short, A. D., Alfonso, A. & Gill, D. L. (1995). A novel Ca^{2+} entry mechanism is turned on during growth arrest induced by Ca^{2+} pool depletion. *Journal of Biological Chemistry* **270**, 26790–26793.

Van Driessche, W., Simaels, J., Aelvoet, I. & Erlij, D. (1988). Cation-selective channels in amphibian epithelia: electrophysiological properties and activation. *Comparative Biochemistry and Physiology* **90**, 693–699.

Van Driessche, W. & Zeiske, W. (1985). Ca^{2+}-sensitive, spontaneously fluctuating, cationic channels in the apical membrane of the adult frog skin epithelium. *Pflügers Archiv* **405**, 250–259.

Vogalis, F., Ward, M. & Horowitz, B. (1995). Suppression of two cloned smooth muscle-derived delayed rectifier potassium channels by cholinergic agonists and phorbol esters. *Molecular Pharmacology* **48**, 1015–1023.

Xiong, Z., Sperelakis, N., Noffsinger, A. & Fenoglio-Preiser, C. (1993). Fast Na^+ current in circular smooth muscle cells of the large intestine. *Pflügers Archiv* **423**, 485–491.

Xiong, Z., Sperelakis, N., Noffsinger, A. & Fenoglio-Preiser, C. (1995). Ca^{2+} currents in human colonic smooth muscle cells. *American Journal of Physiology* **269**, G378–385.

ZHANG, Y., MCBRIDE, D. W. JR & HAMILL, O. P. (1998). The ion selectivity of a membrane conductance inactivated by extracellular calcium in *Xenopus* oocytes. *Journal of Physiology* **508**, 763–776.

ZHOLOS, A. V. & BOLTON, T. B. (1994). G-protein control of voltage dependence as well as gating of muscarinic metabotropic channels in guinea-pig ileum. *Journal of Physiology* **478**, 195–202.

ZHOLOS, A. V. & BOLTON, T. B. (1995). Effects of divalent cations on muscarinic receptor cationic current in smooth muscle from guinea-pig small intestine. *Journal of Physiology* **486**, 67–82.

Acknowledgements

This work was supported by grant number 051162/Z from The Wellcome Trust.

Corresponding author

T. B. Bolton: Department of Pharmacology and Clinical Pharmacology, St George's Hospital Medical School, London SW17 0RE, UK.

Email: t.bolton@sghms.ac.uk